Philosophical Magazine

ISSN: 1478-6435 (Print) 1478-6443 (Online) Journal homepage: https://www.tandfonline.com/loi/tphm20

Effect of a buffer layer between the shell and ligand on the optical properties of an exciton and biexciton in type-II quantum dot nanocrystals

Fatih Koç, Koray Koksal & Mehmet Sahin

To cite this article: Fatih Koç, Koray Koksal & Mehmet Sahin (2017) Effect of a buffer layer between the shell and ligand on the optical properties of an exciton and biexciton in type-II quantum dot nanocrystals, Philosophical Magazine, 97:3, 201-211, DOI: 10.1080/14786435.2016.1252861

To link to this article: https://doi.org/10.1080/14786435.2016.1252861

PHILOSOPHICAL MAGAZINE, 2017
VOL. 97, NO. 3, 201–211
http://dx.doi.org/10.1080/14786435.2016.1252861

Taylor & Francis
Taylor & Francis Group

Effect of a buffer layer between the shell and ligand on the optical properties of an exciton and biexciton in type-II quantum dot nanocrystals*

Fatih Koç[a,b], Koray Koksal[b] and Mehmet Sahin[c]

[a]Faculty of Sciences, Department of Physics, Selcuk University, Konya, Turkey; [b]Department of Material Science, Bitlis Eren University, Bitlis, Turkey; [c]Department of Material Science and Nanotechnology Engineering, Abdullah Gül University, Kayseri, Turkey

ABSTRACT

In this study, we have investigated the effect of the buffer layers on the electronic and optical properties of an exciton (*X*) and a biexciton (*XX*) in a type-II CdTe/CdSe quantum dot nanocrystal. In an experimental study, it has been reported that when a CdTe/CdSe quantum dot nanocrystal is coated by a ZnTe material as a buffer layer, the photoluminescence quantum yield is growing from 4 to 20%. We have confirmed theoretically this improvement and extended the calculations to an *XX* structure. In the calculations, two different semiconductor materials, CdS and ZnTe, have been considered for the buffer layer. We have theoretically shown that the buffer layer causes an increase in the radiative oscillator strength of both *X* and *XX*. When the ZnTe is used as the buffer layer, the oscillator strength becomes stronger when compared to CdSe buffer material because of higher conduction band offset between CdSe and ZnTe.

ARTICLE HISTORY
Received 7 June 2016
Accepted 19 October 2016

KEYWORDS
Quantum dot; type-II nanocrystals; multi-exciton in nanocrystals

1. Introduction

The possibility of manipulating and tuning the properties of confined electrons and holes in nanosize semiconductor quantum dot nanocrystals (QDNCs) is the subject of a great interest due to its potential applications in photovoltaic devices [1–3]. There are two basic principles of tuning the quantum mechanical properties of the QDNCs which are the variation of the size of the core/shell layers [4] and the change of the using materials in core/shell region [5]. Another process for changing the properties of the semiconductor QDNC is to separate and confine the electron and hole in different regions as in the case of type-II QDNCs [1,6]. This spatial separation of the carriers provides a great advantages such as band bending effect [7,8], long radiative lifetime [9] and large optical anisotropy [10,11].

There are some differences between type-I and type-II semiconductor QDNCs. As a novel property of the type-II semiconductor QDNCs, the value of the effective band gap [1] can be modulated which means that it is possible to separately tune the energy levels

CONTACT Mehmet Sahin mehmet.sahin@agu.edu.tr
*This work is a part of the MSc degree thesis prepared by F. Koç at Physics Department of Selcuk University.

of electron(s) and hole(s) by changing the size of the shell and core layers. This novelty is not available in type-I semiconductor QDNCs. Therefore, it is possible to obtain long excitonic radiative life time [12] in type-II QDNCs. Emission properties are also sensitive to the size of the core and shell materials [13]. Furthermore, in contrast to type-I QDNCs, the excitation of single excitons can be sufficient for optical gain in type-II QDNCs [14].

A number of experimental and theoretical studies on the electronic and optical properties of excitons in type-II quantum dots has been reported in the literature [1,4,13, 15–18]. The effects of the shell thickness and core size on the electronic and optical properties have been also investigated recently. Particularly, the exciton dynamics in type-II structures has been researched due to their importance in the solar cell applications. As well known, a biexciton in a QDNC is the simplest multiexciton structure. However, the theoretical discussions on the *XX* dynamics are not sufficient to understand the multiexciton mechanism in type-II quantum dots. The studies on the effect of the layers of QDNCs have been limited to the core/shell type-II semiconductor quantum dots [15]. But, it is also possible to grow this kind of systems in the form of multi-shell structures. The researches on the multi-shell type-I semiconductor QDNCs have shown that the presence of multi-layers provide a flexibility to tune the quantum mechanical properties of the structure [19,20]. In order to understand the effect of multi-layers on the single and multiexciton in type-II structures, still theoretical and experimental effort is required.

In this work, we concentrate on the optical properties of single excitons and biexcitons in type-II semiconductor QDNCs. The main aim of this study is to calculate for the first time the effect of buffer material between the shell layer and ligand on the electronic and optical properties of an exciton and to compare the results with that of experimental work of Kim et al. [1]. The calculation is also expanded to a biexciton complex in the same structure. The optical properties such as overlap integral, absorption wavelength, binding energy, oscillator strength and lifetime of the *X* and *XX* in the QDNC heterostructures are investigated for different buffer materials (CdS and ZnTe) and for different shell thicknesses. The results are discussed in the light of the possible physical reasons behind the electronic and optical properties.

2. Model and theory

We consider a spherically symmetric type-II CdTe/CdSe/buffer/ligand (i.e. core/shell/buffer/ligand) QDNC. In this structure, hole is localised in the CdTe core region while electron is localised in the CdSe shell one. Figure 1 shows the potential profile of CdTe/CdSe/CdS and CdTe/CdSe/ZnTe structures. In the first structure, CdS is chosen as the buffer layer while ZnTe is used instead of the CdS in the second structure. In the calculations, the thicknesses of the buffer layers are set to 0.1 a_0.

In the effective mass approximation and BenDaniel–Duke boundary conditions, the single particle Schrödinger equations of a multi-exciton complex can be written as

$$\left[-\frac{\hbar^2}{2}\vec{\nabla}_r\left(\frac{1}{m_e^*(r)}\vec{\nabla}_r\right)+V_e(r)-q_e\Phi_h+q_e\Phi_e+V_{xc}^{e-e}[\rho_e(r)]\right]R_e(r)=\varepsilon_e R_e(r), \quad (1)$$

and

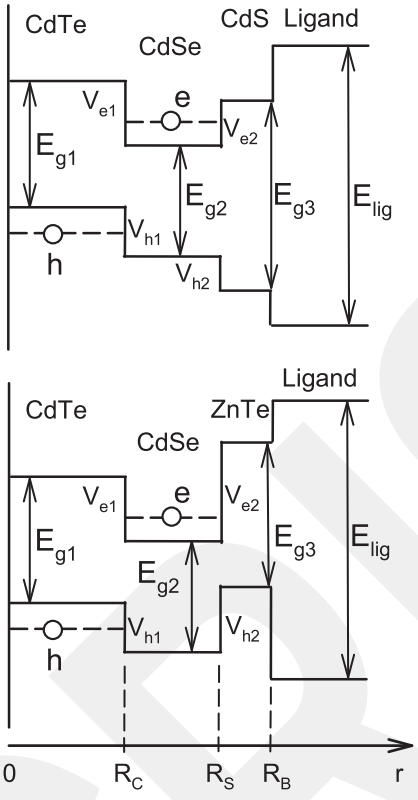

Figure 1. Potential profile of the CdTe/CdSe quantum dot structures. The buffer materials are chosen as CdS in the upper panel, and as ZnTe in the bottom panel.

$$\left[-\frac{\hbar^2}{2}\vec{\nabla}_r\left(\frac{1}{m_h^*(r)}\vec{\nabla}_r\right)+V_h(r)-q_h\Phi_e+q_h\Phi_h+V_{xc}^{h-h}[\rho_h(r)]\right]R_h(r)=\varepsilon_h R_h(r), \quad (2)$$

where $\hbar$ is the reduced Planck's constant, $m_e^*(r)$ and $m_h^*(r)$ are the position dependent effective mass of the electron and hole, respectively, $V_e(r)$ is the electron confinement potential and $V_h(r)$ is the hole confinement potential, q_e and q_h are charges of the electron and hole, respectively, and Φ_e and Φ_h are the electrostatic Coulomb potentials of the electron and hole, respectively. The $V_{xc}[\rho(r)]$ potentials are the exchange-correlation potentials between the same kinds of particles, and $R_e(r)$ and $R_h(r)$ are the radial part of the electron and hole wave functions, respectively. ε_e is the energy eigenvalue of the electron and similarly, ε_h is the hole energy.

These two equations coupled by means of the attractive Coulomb terms, $q_e\Phi_h$ and $q_h\Phi_e$. Equations (1) and (2) must be solved simultaneously and self-consistently. The self-consistency requirement in the calculations has been provided through the repulsive Coulomb potentials, $q_e\Phi_e$ and $q_h\Phi_h$. As a result, all Coulomb effects on the energy eigenvalues and wavefunctions have been taken into account. The all Coulomb potentials are calculated from the Poisson equations

$$\vec{\nabla}\kappa(r)\vec{\nabla}\Phi_e=\frac{q_e}{\varepsilon_0}\rho_e(r)$$

$$\vec{\nabla}\kappa(r)\vec{\nabla}\Phi_h = -\frac{q_h}{\varepsilon_0}\rho_h(r), \tag{3}$$

where ρ_e and ρ_h are the density [16] of the electron and hole, respectively, ε_0 is dielectric permittivity of the vacuum and $\kappa(r)$ is the position dependent dielectric constant of the structure. These equations contain the image potential contributions due to surface polarisation at the interfaces.

It should be noted that the position dependent effective masses and dielectric constants are

$$m^*_{e,h}(r) = \begin{cases} m^*_{e,h}(CdTe), & r < R_C \\ m^*_{e,h}(CdSe), & R_C < r < R_S \\ m^*_{e,h}(buff), & R_S < r < R_B \\ m^*_{e,h}(lig), & r > R_B \end{cases}, \quad \kappa(r) = \begin{cases} \kappa(CdTe), & r < R_C \\ \kappa(CdSe), & R_C < r < R_S \\ \kappa(buff), & R_S < r < R_B \\ \kappa(lig), & r > R_B \end{cases}. \tag{4}$$

In self-consistent Poisson–Schrödinger calculations, these effective mass values have been used in the frame of the BenDaniel–Duke boundary conditions.

In single exciton case, repulsive Coulomb and the exchange-correlation terms, i.e. last two terms of the left-hand side of Equations (1) and (2), are ignored due to a single electron and hole. Perdew and Zunger [21] expression, which is a parametrisation of the Monte Carlo results of Ceperley and Alder [22], is employed for the exchange-correlation potential of the XX. This formulation contains the self-interaction correction.

The last three equations, Equations (1)–(3), should be solved self-consistently. For this purpose, the full numeric matrix diagonalisation technique is used in a real-space. The details of the calculation schemes can be seen in Ref. [15].

The binding energy of XX is described as [17]

$$E_b^{XX} = E_{XX}^{tot} - 2E_X^{tot}, \tag{5}$$

where E_X^{tot} is single exciton total energy, and E_{XX}^{tot} is biexciton total energy.

Being a unitless parameter, the oscillator strength, which is a measure of optical transitions, is very important in studying of all optical properties of any quantum structures. The single exciton oscillator strength is expressed as [23]

$$f_X = \frac{E_p}{2E_X}\left|\int r^2 \mathrm{d}r R_e(r)R_h(r)\right|^2, \tag{6}$$

where E_p is the Kane energy, E_X is the exciton transition energy, $R_e(r)$ and $R_h(r)$ are the radial part of electron and hole wavefunctions, respectively.

The recombination oscillator strengths of the XX are calculated by means of

$$f_{XX} = A\frac{E_p}{2E_{XX}}\left|\int r^2 \mathrm{d}r R_e(r)R_h(r)\right|^2, \tag{7}$$

where E_{XX} is the biexciton transition energy, $R_e(r)$ and $R_h(r)$ are the radial part of the electron and hole wavefunctions of the XX. Here, the A is a recombination probability and the factor $A \simeq 4$ for bound and $A \simeq 2$ for unbound XXs. The details of this approximation can be found in Ref. [19].

Table 1. The material parameters used in the calculations.

Material	m_e^*/m_0	m_h^*/m_0	κ	E_g	V_e (eV)	V_h (eV)
CdTe	0.096 [18]	0.4 [18]	10.4 [30]	1.61 [29]	(CdTe–CdSe) 0.42 [29]	(CdTe–CdSe) 0.57 [29]
CdSe	0.12 [18]	0.45 [18]	9.29 [30]	1.76 [29]	(CdSe–CdS) 0.32 [29]	(CdSe–CdS) 0.42 [29]
CdS	0.2 [30]	0.7 [30]	8.73 [30]	2.50 [29]	(CdSe–ZnTe) 1.22 [14]	(CdSe–ZnTe) 0.7 [14]
ZnTe	0.122 [30]	0.6 [30]	10.3 [30]	2.26 [31]	(CdS–Ligand) 2.75	(CdS–Ligand) 2.75
Ligand	1.0 [18]	1.0 [18]	2.0 [18]	8.0 [18]	(ZnTe–Ligand) 2.87	(ZnTe–Ligand) 2.87

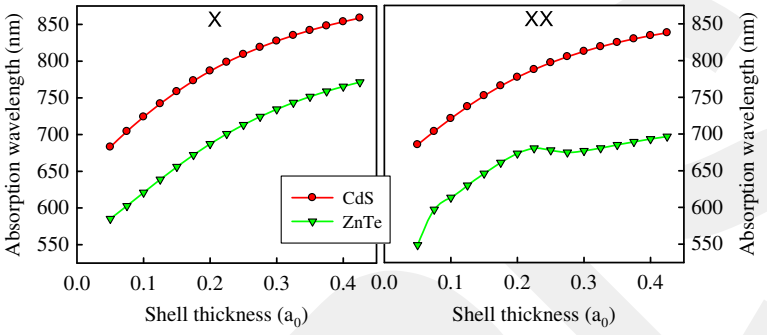

Figure 2. (colour online) Absorption wavelength of the *X* (left panel) and *XX* (right panel) structures as a function of the CdSe shell thickness.

The radiative lifetime of excitonic structures is an important quantity and therefore a number of studies on lifetime have been reported both theoretically and experimentally [6,24–26]. The radiative lifetime is inversely proportional with the oscillator strength and it is given as [27,28]

$$\tau = \frac{6\pi\varepsilon_0 m_0 c^3 \hbar^2}{e^2 n \beta_s E^2 f}, \tag{8}$$

where ε_0 is the dielectric permittivity of the vacuum, m_0 is the free electron mass, c is the light velocity, e is the electronic charge, f is the oscillator strength, n is the refractive index, E is the transition energy and β_s is the screening factor [28].

3. Results and discussion

We have used the atomic units throughout the calculations, where the Planck constant $\hbar = m_0 = e = 1$. The material parameters used in the calculations are listed in Table 1. The effective exciton Bohr radius and the Rydberg energy are calculated as $a_0 = 71.06$ Å and $R_y = 9.74$ meV, respectively, in terms of the CdTe material parameters. In our considered core/shell structure CdTe/CdSe, hole resides in CdTe core region, whereas electron is confined in CdSe shell one and here, the core radius has been set to $R_1 = 1.95$ nm.

In Figure 2, the changes of the absorption wavelength, which correspond to transition energy, are shown for the *X* (left panel) and *XX* (right panel) as a function of the CdSe shell thickness. As seen from the figures, in all cases, absorption wavelengths grow (or transition energies reduce) with increasing of the shell thicknesses. This is an expected result because the energy levels are inverse proportional to the size of the quantum structures. As reported in the literature, in type-I core/shell or single core structures, the exciton transition energy

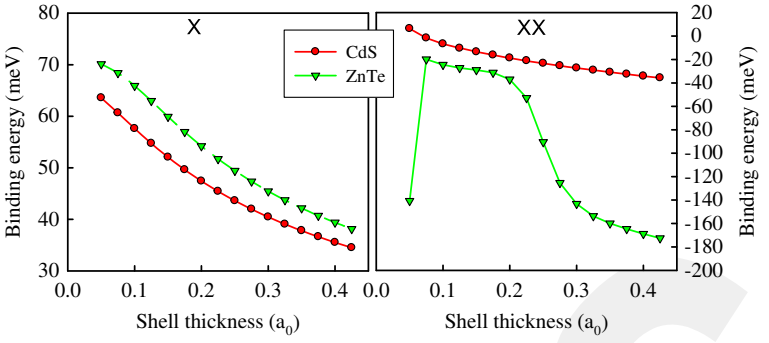

Figure 3. (colour online) Potential profile of the CdTe/CdSe quantum dot structures. The buffer materials are chosen as CdS in the left panel, and as ZnTe in the right panel.

is larger than that of the biexciton [20,32,33]. Yet, in the type-II structures, as seen from the figures, the absorption wavelength of the *X* is larger than that of the *XX*. This means that the transition energy of the *X* is smaller in type-II structures than in type-I ones. These results are in a good agreement with experimental studies [14,35]. Contrary to type-I, in type-II structures since the electrons and holes are confined in the different spatial region, the repulsive Coulomb interaction become more effective in the *XX* structures and so the transition energies become larger. On the other hand, in an exciton structure, although there is no a repulsive interaction in both type-I and type-II structures, the attractive Coulomb interaction in the type-II structures is smaller when compared to that in the type-I. The buffer material has an important influence on the absorption wavelength. As seen from the figures, when CdS is chosen as the buffer layer, the absorption wavelength goes to larger values when compared with the structure that has ZnTe buffer layer. The physical reason of this can be explained as follows: because the electron confining potential formed by CdS is smaller than that of ZnTe, the electron penetration into the CdS becomes much more in comparison to the penetration into the ZnTe. So, the energy levels become smaller in the first case and this leads to higher absorption wavelengths in both the *X* and *XX* structures. While, in the case of CdS buffer, the absorption wavelengths of the *X* and *XX* increase monotonously with increasing CdSe shell thicknesses, in CdTe/CdSe/ZnTe quantum dot heterostructure, the absorption wavelength of the *XX* is non-monotonous. The physical origin of this behaviour can be explained by means of the potential profile of the structure. As can be seen from the bottom panel of Figure 1, the valence band edge becomes higher when compared to that of the core one and in small shell thicknesses the holes are much more affected from this potential region until a certain thickness value of the shell. On the other hand, in addition to this effect in the valence band, while the shell thickness increases, the repulsive Coulomb interaction decreases between the electrons. All of these changes derivate the absorption wavelength of the *XX* from monotonous behaviour in the case of ZnTe layer.

In Figure 3, the binding energies of the *X* (left panel) and *XX* (right panel) are given depending on the CdSe shell thickness. In the case of the *X*, as can be seen from the left panel of the figure, the binding energies are positive, namely bound exciton structure, in both ZnTe, and CdS buffer layer cases and decrease with increasing shell layer thicknesses. These are typical exciton binding energy behaviours in a quantum dot heterostructures.

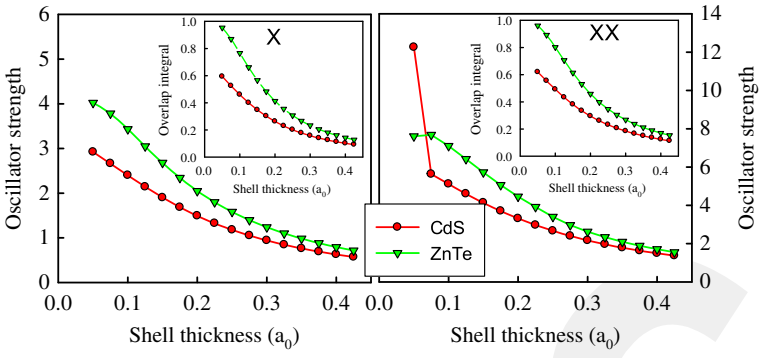

Figure 4. (colour online) The recombination oscillator strength of the *X* (left panel) and *XX* (right panel) as a function of the CdSe shell thickness. Insets show the overlap integral of the wavefunctions of the same structures.

On the other hand, the binding energy of the *X* in case of the ZnTe buffer material is larger than that of the CdS buffer material case. This is because the confinement of the electron is so strong in the first case. In the case of *XX* with CdS coating for buffer layer, we observed that when the shell thickness is smaller 0.1 a_0, the binding energy becomes positive (bounded biexciton), but in larger values of the shell thicknesses than the 0.1 a_0, the binding energy becomes negative (i.e. unbounded biexciton). General behavior of the binding energy is smooth decreasing tendency. In CdTe/CdSe/ZnTe heterostructure, the binding energy of the *XX* calculated as ≈ -140 meV as the shell thickness is 0.05 a_0. This observation can be explained as follows: As seen from the potential profile in Figure 1, in very thin shell layer, while the holes energy levels decrease due to lower confinement potential of the ZnTe buffer layer, the electrons are forced to confine to smaller CdTe core region. As a result, the repulsive Coulomb interaction and the kinetic energies of the electrons will become larger and so the total energy value of the electrons becomes higher. In the case of shell thickness values from 0.075 a_0 to 0.225 a_0, the binding energy of *XX* exhibits a smooth decreasing. In this case, the electrons do not confine completely to the CdSe shell. That is, the electron density expands throughout the CdTe/CdSe structure and the repulsive Coulomb interaction between the electron becomes smaller. When the shell thickness becomes greater than 0.225 a_0, it is observed that the binding energy exhibits a sharply decrease behaviour. The reason of this behaviour is that the electrons confine to the CdSe shell region and consequently, the repulsive Coulomb interaction, which reduces the binding energy, between the electrons becomes larger. The binding energy has a smooth decreasing tendency with further increasing of the shell thickness.

Figure 4 shows the recombination oscillator strengths and overlap integrals of the *X* (left panel) and *XX* (right panel) as a function of the CdSe layer thickness. As seen from the figures, the oscillator strengths decrease with increasing of the CdSe layer thicknesses in all cases. These behaviours are very similar to the overlap integrals of the wavefunctions as can be seen from the insets. In the first structure, labelled as CdTe/CdSe/CdS, the spatial separation of the carriers become higher due to the moving of the electron density towards the CdS layer. Hence, even if the layer thickness of CdSe is very thin, the overlap integral experiences small values in both *X* and *XX* cases and the overlap integral values lie in the

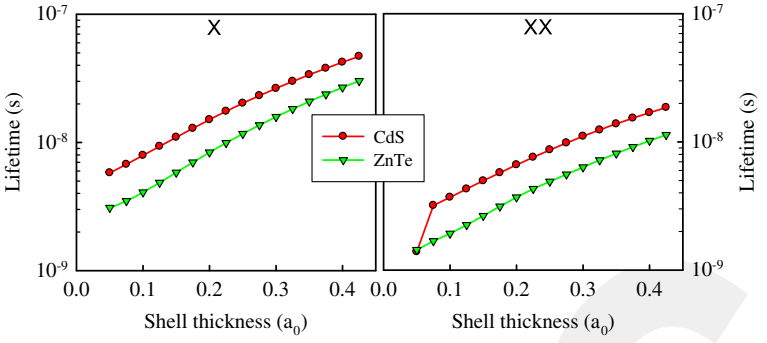

Figure 5. (colour online) The radiative lifetime of the *X* and *XX* as a function of the CdSe shell thickness.

range of 0.1 and 0.6 in the first structure. As a result of this weak overlaps, the oscillator strengths in the first structure become smaller. In this structure, because the *XX* become bound, its oscillator strength is approximately four times greater than that of *X* when shell thickness is 0.05 a_0. On the other side, in other considered structure, CdTe/CdSe/ZnTe, the electron confining potential originated from the ZnTe layer is higher than that of the CdTe and hence, this case brings about to localise of electron(s) to the core region or blocks the penetration of the electron into the ligand in small CdSe shell thicknesses. Hence, the overlap integrals of both *X* and *XX* have larger values when we compared to the former structure. Using the buffer layer increases the overlap of the wavefunctions and for that reason, the photoluminescence quantum yield (PLQY) becomes higher than that of the case without buffer layers as is reported experimentally by Kim et al. [1] They show that the PLQY can raise from 4 up to 20% if the CdTe/CdSe type-II QD is coated by ZnTe. In small shell thicknesses, the wavefunction of the electron(s) expands to whole structure. In this case, the structure called as quasi-type II and the overlap of the wavefunctions become larger as seen from the insets. The values of the overlap integral take between the range of 0.15 and almost 1.0. This strong overlap causes the strong oscillator strength. When the shell thickness is very thin (0.05 a_0), depending on the energy difference between the initial and final states, the oscillator strength of the *XX* becomes almost two times greater than that of the shell thickness is 0.1 a_0.

Figure 5 shows the radiative lifetimes of the *X* (left panel) and *XX* (right panel) as a function of the CdSe shell thickness in CdTe/CdSe/CdS and CdTe/CdSe/ZnTe structures. The lifetimes increase with increasing of the CdSe shell thicknesses owing to the decreasing of the overlap as can be expected in all cases. In CdTe/CdSe/CdS structure, due to lower oscillator strengths and transition energies, the radiative lifetimes of the *X* and *XX* are higher than that of the other structure include ZnTe buffer layer. In general, it is expected that type-II QDNCs have longer exciton decay times than type-I QDNCs [12] because of the spatial separation of charges. Thanks to this feature, type-II structures are made more suitable for the photovoltaic applications since the carriers may separate before their recombination.

4. Conclusion

In the study, we have investigated the electronic and optical properties of a single exciton and biexciton in a CdTe/CdSe type-II QDNCs which include a thin buffer layer between the shell and ligand. Poisson and Schrodinger equations have been solved self-consistently in the Hartree approximation to obtain energy levels and corresponding wavefunctions. In biexciton calculations, we have taken into account the quantum mechanical many-particle effects in the local density approximation. The optical properties, absorption wavelengths, overlap integrals, oscillator strengths and radiative lifetimes, have been carried out using the wavefunctions and energy values obtained. In the calculations, two different materials, CdS and ZnTe, have been considered as the buffer layer. We show that the buffer layer plays drastically important role on the optical properties of the X and XX and both of materials increase the oscillator strength. When we compare the effect of CdS and ZnTe, it is seen that the ZnTe used as the buffer layer, the overlaps of the wavefunctions become stronger in comparison to CdS. We conclude that if a type-II nanocrystals are used for fabrication of an optoelectronic devices, such as an LED, covering of the type-II nanocrystal with a buffer layer will become more efficient of the device performance. Finally, it should be noted that an increase in the shell thickness of II-VI core-shell well QDs leads to the increase in lifetime as reported in a recent experimental study [36] which is consistent with our theoretical results.

Acknowledgement

MS thanks Abdullah Gul University Foundation (AGUV) for their partial financial support.

Disclosure statement

No potential conflict of interest was reported by the authors.

Funding

This work was supported by the TUBITAK TBAG [project number 109T729].

References

[1] S. Kim, B. Fisher, H.-J. Eisler, and M. Bawendi, *Type-II quantum dots: CdTe/CdSe(core/shell) and CdSe/ZnTe(core/shell) heterostructures*, J. Am. Chem. Soc. 125 (2003), pp. 11466–11467.
[2] V.P. Kamat, *Quantum dot solar cells. Semiconductor nanocrystals as light harvesters*, J. Phys. Chem. C 112 (2008), pp. 18737–18753.
[3] X. Peng, L. Manna, W. Yang, J. Wickham, E. Scher, A. Kadavanich, and A.P. Alivisatos, *Shape control of CdSe nanocrystals*, Nature 404 (2000), pp. 59–61.
[4] J. Bang, J. Park, J.H. Lee, N. Won, J. Nam, J. Lim, B.Y. Chang, H.J. Lee, B. Chon, J. Shin, J.B. Park, J.H. Choi, K. Cho, S.M. Park, T. Joo, and S. Kim, *ZnTe/ZnSe (core/shell) type-II quantum dots: Their optical and photovoltaic properties*, Chem. Mater. 22 (2009), pp. 233–240.
[5] P. Reiss, M. Protiere, and L. Li, *Core/shell semiconductor nanocrystals*, Small 5 (2009), pp. 154–168.
[6] S.A. Ivanov and M. Achermann, *Spectral and dynamic properties of excitons and biexcitons in type-II semiconductor nanocrystals*, ACS Nano 4 (2010), pp. 5994–6000.

[7] M. Larsson, A. Elfving, P.O. Holtz, G.V. Hansson, and W.X. Ni, *Spatially direct and indirect transitions observed for Si/Ge quantum dots*, Appl. Phys. Lett. 82 (2003), pp. 4785–4787.
[8] Y.S. Chiu, M.H. Ya, W.S. Su, and Y.F. Chen, *Properties of photoluminescence in type-II GaAsSb/GaAs multiple quantum wells*, J. Appl. Phys. 92 (2002), pp. 5810–5813.
[9] F. Hatami, M. Grundmann, N.N. Ledentsov, F. Heinrichsdorff, R. Heitz, J. Bohrer, D. Bimberg, S.S. Ruvimov, P. Werner, V.M. Ustinov, P.S. Kopev, and Zh. I. Alferov, *Carrier dynamics in type-II GaSb/GaAs quantum dots*, Phys. Rev. B 57 (1998), pp. 4635–4641.
[10] S.V. Zaitsev, A.A. Maksimov, V.D. Kulakovskii, I.I. Tartakovskii, D.R. Yakovlev, W. Ossau, L. Hansen, and G. Landwehr, *Interface properties and in-plane linear photoluminescence polarization in highly excited type-II ZnSe/BeTe heterostructures with equivalent and nonequivalent interfaces*, J. Appl. Phys. 91 (2002), pp. 652–657.
[11] C.H. Wang, *T.-Te Chen, Y. F. Chen, M. L. Ho, C. W. Lai, P. T. Chou, Recombination dynamics in CdTe/CdSe type-II quantum dots*, Nanotechnology 19 (2008), pp. 115702-1–115702-6.
[12] F. Hatami, M. Grundmann, N.N. Ledentsov, F. Heinrichsdorff, R. Heitz, J. Bohrer, D. Bimberg, S.S. Ruvimov, P. Werner, V.M. Ustinov, P.S. Kopev, and Z.I. Alferov, *Carrier dynamics in type-II GaSb/GaAs quantum dots*, Phys. Rev. B 57 (1998), pp. 4635–4641.
[13] V.I. Klimov, S.A. Ivanov, J. Nanda, M. Achermann, I. Bezel, J.A. McGuire, and A. Piryatinski, *Single-exciton optical gain in semiconductor nanocrystals*, Nature 447 (2007), pp. 441–446.
[14] J. Nanda, S.A. Ivanov, M. Achermann, I. Bezel, A. Piryatinski, and V.I. Klimov, *Light amplification in the single-exciton regime using exciton–exciton repulsion in Type-II nanocrystal quantum dots*, J. Phys. Chem. C 111 (2007), pp. 15382–15390.
[15] F. Koc and M. Sahin, *Electronic and optical properties of single excitons and biexcitons in type-II quantum dot nanocrystals*, J. Appl. Phys. 115 (2014), pp. 193701-1–193701-10.
[16] M. Sahin, S. Nizamoglu, O. Yerli, and H.V. Demir, *Reordering orbitals of semiconductor multi-shell quantum dot-quantum well heteronanocrystals*, J. Appl. Phys. 111 (2012), pp. 023713-1–023713-6.
[17] T. Tsuchiya, *Biexcitons and charged excitons in quantum dots: A quantum monte carlo study*, Physica E 7 (2000), pp. 470–474.
[18] E.J. Tyrrell and J.M. Smith, *Effective mass modeling of excitons in type-II quantum dot heterostructures*, Phys. Rev. B 84 (2011), pp. 165328-1–165328-12.
[19] M. Sahin and F. Koc, *A model for the recombination and radiative lifetime of trions and biexcitons in spherically shaped semiconductor nanocrystals*, Appl. Phys. Lett. 102 (2013), pp. 183103-1–183103-4.
[20] A. Akturk, M. Sahin, F. Koc, and A. Erdinc, *A detailed investigation of electronic and optical properties of the exciton, the biexciton and charged excitons in a multi-shell quantum dot nanocrystal*, J. Phys. D: Appl. Phys. 47 (2014), pp. 285301-1–285301-13.
[21] J.P. Perdew and A. Zunger, *Self-interaction correction to density-functional approximations for many-electron systems*, Phys. Rev. B 23 (1981), pp. 5048–5079.
[22] D.M. Ceperley and B.J. Alder, *Ground state of the electron gas by a stochastic method*, Phys. Rev. Lett. 45 (1980), pp. 566–568.
[23] V.A. Fonoberov and A.A. Balandin, *Excitonic properties of strained wurtzite and zinc-blende GaN/AlxGa1xNGaN/AlxGa1xN quantum dots*, J. Appl. Phys. 94 (2003), pp. 7178–7186.
[24] M. Gong, W. Zhang, G.C. Guo, and L. He, *Atomistic pseudopotential theory of optical properties of exciton complexes in InAs/InP quantum dots*, Appl. Phys. Lett. 99 (2011), pp. 231106-1–231106-3.
[25] P.P. Jha and P. Guyot-Sionnest, *Trion decay in colloidal quantum dots*, ACS Nano 3 (2009), pp. 1011–1015.
[26] G.A. Narvaez, G. Bester, and A. Zunger, *Excitons, biexcitons, and trions in self-assembled (In, Ga) As Ga As quantum dots: Recombination energies, polarization, and radiative lifetimes versus dot height*, Phys. Rev. B 72 (2005), pp. 245318-1–245318-10.
[27] M. Califano, A. Franceschetti, and A. Zunger, *Lifetime and polarization of the radiative decay of excitons, biexcitons, and trions in CdSe nanocrystal quantum dots*, Phys. Rev. B 75 (2007), pp. 115401-1–115401-7.

[28] B. Alen, J. Bosch, D. Granados, J. Martinez-Pastor, J.M. Garcia, and L. Gonzalez, *Oscillator strength reduction induced by external electric fields in self-assembled quantum dots and rings*, Phys. Rev. B 75 (2007), pp. 045319-1–045319-7.
[29] S.-H. Wei, S. B. Zhang, and A. Zunger, *First-principles calculation of band offsets, optical bowings, and defects in CdS, CdSe, CdTe, and their alloys*, J. Appl. Phys. 87 (2000), pp. 1304–1311.
[30] O. Madelung, *Semiconductors: Data Handbook*, Springer, Heidelberg, 2004.
[31] C.Y. Chen, C.T. Cheng, C.W. Lai, Y.H. Hu, P.T. Chou, Y.H. Chou, and H.T. Chiu, *Type II CdSe/CdTe/ZnTe (core–shell–shell) quantum dots with cascade band edges: The separation of electron (at CdSe) and hole (at ZnTe) by the CdTe layer*, Small 1 (2005), pp. 1215–1220.
[32] Y. Louyer, L. Biadala, J.-B. Trebbia, M.J. Fernée, Ph Tamarat, and B. Lounis, *Efficient biexciton emission in elongated CdSe/ZnS nanocrystals*, Nano Lett. 11 (2011), pp. 4370–4375.
[33] B. Patton, W. Langbein, and U. Woggon, *Trion, biexciton, and exciton dynamics in single self-assembled CdSe quantum dots*, Phys. Rev. B 68 (2003), pp. 125316-1–125316-9.
[34] A. Akturk, H. Tas, K. Koksal, and M. Sahin, *The electronic and optical properties of a triexciton in CdSe/ZnS core/shell quantum dot nanocrystals*, Philos. Mag. 96 (2016), pp. 584–595.
[35] K. Matsuda, S.V. Nair, H.E. Ruda, Y. Sugimoto, T. Saiki, and K. Yamaguchi, *Two-exciton state in GaSb/GaAs type-II quantum dots studied using near-field photoluminescence spectroscopy*, Appl. Phys. Lett. 90 (2007), pp. 013101-1–013101-3.
[36] C.M. Tyrakowski, A. Shamirian, C.E. Rowland, H. Shen, A. Das, R.D. Schaller, and P.T. Snee, *Bright Type II quantum dots*, Chem. Mater. 27 (2015), pp. 7276–7281.